Correct space group determination of 2D materials

Rashmi Ranjan Routaray [1,2] Eric Bousquet [2] Matteo Giantomassi [1] and Xavier Gonze [1]
[1]*European Theoretical Spectroscopy Facility, Institute of Condensed Matter and Nanosciences, Université Catholique de Louvain, Chemin des étoiles 8, bte L07.03.01, B-1348 Louvain-la-Neuve, Belgium*
[2]*Physique Théorique des Matériaux, Q-MAT, Université de Liège, B-4000 Sart-Tilman, Belgium*

(Received 11 April 2025; accepted 26 June 2025; published 27 August 2025)

Two-dimensional (2D) materials, such as monolayer CrI_3, are the focus of much attention because of their unique properties and potential applications in various technological fields. Despite their discovery years ago, there remains significant confusion regarding space group assignments, with disparities reported across well-known 2D material databases and publications. Therefore, accurate determination of space groups is crucial for understanding the intrinsic properties of these materials and optimizing their performance. We use first-principles calculations to systematically investigate the space group of monolayer CrI_3 and other 2D materials reported with disparities. From total energy, geometry optimization, and subsequent lattice dynamics computations, we identify common sources of confusion and propose a methodology to resolve these ambiguities. Our results highlight the necessity of integrating computational analyses with symmetry analysis to achieve a correct space group determination of 2D materials. This approach can be beneficial for, e.g., machine learning algorithms that rely on accurate determination of crystal symmetry to identify material properties.

DOI: 10.1103/dj5c-d24m

I. INTRODUCTION

The discovery of graphene [1] by A. Geim and K. Novoselov in 2004 led to a significant interest in the field of two-dimensional (2D) materials. Graphene's extraordinary electrical, thermal and mechanical properties [2,3] showcased the immense potential of 2D materials in a variety of applications, ranging from electronics to energy storage. This important discovery triggered a wave of interest, inspiring the materials research community to investigate a wide variety of 2D materials with unique properties and promising technological applications [4,5].

Despite rapid advancements, one persistent challenge in this field of 2D materials has been the study of magnetism. For a long time, intrinsic magnetism in an atomic thin layer was elusive [6] until the breakthrough with monolayer (ML) CrI_3 [7], the first 2D material to exhibit stable magnetic ordering. This exceptional magnetic property at the atomic scale opened new avenues for research in spintronics and other advanced applications. Since the discovery of magnetism in ML CrI_3, a significant amount of research has been dedicated to exploring its potential applications [8–10] and understanding its underlying mechanisms. However, as we discuss below, the accurate determination of space groups in 2D materials, including ML CrI_3, remains problematic, with significant disparities reported in various databases and scientific publications.

We found that ML CrI_3 is documented with conflicting space groups, $P\bar{3}$ and $P\bar{3}1m$, in the Materials Cloud two-dimensional crystals database (MC2D) [11] and the Computational 2D Materials Database (C2DB) [12], respectively. These well-known databases produce the structures by cleaving layers from the bulk material structure.

Similarly, diverse reports in the scientific literature further compound this ambiguity, including C2/m [13] and $P\bar{3}1m$ [14] space groups.

During our early investigation on ML CrI_3, we encountered similar disparities in the space group assignments of other ML materials [15], including $CrGeTe_3$ [16], $CrSiSe_3$ [17], $CrSiTe_3$ [18], $MnPS_3$ [19], $MnPSe_3$ [20], $NiPS_3$ [21,22], $NiPSe_3$ [23,24], $CrBr_3$ [25,26], $CrCl_3$ [27], CrS_2 [28,29], $CrTe_2$ [30,31], VS_2 [32], VSe_2 [33], and VTe_2 [34].

These disparities hinder a thorough understanding of the structural arrangements of these materials and make it challenging to integrate them seamlessly into advanced technologies. Furthermore, the use of high-throughput computations to identify materials for particular properties like multiferroicity, altermagnetism, flexoelectricity, magnetoelectricity, and optical properties etc. [35–43] or the use of an incorrect space group as input for machine learning models to predict properties, can result in significant errors and unreliable results, making material research and applications even more challenging.

Given these challenges, the present study aims to address the complexities of space-group classifications for these 2D materials. We provide insights to clarify their structural symmetries and improve their use in various technological applications. The article is organized as follows. Section II summarizes the issues with the recognition of space group of the materials at the level of both theory and experiments. Section III details the computational parameters and techniques used in our study. Section IV discusses the results and precautions that should be taken when dealing with different types of 2D materials before concluding in Sec. V.

II. CHALLENGES

Experimental techniques, such as x-ray diffraction (XRD) and electron microscopy, often struggle with the reduced dimensionality and surface effects inherent in 2D materials,

leading to ambiguous or conflicting results. Sample quality, substrate interactions, and measurement sensitivity can further complicate the interpretation of diffraction patterns, resulting in varied space group assignments [44,45].

One might expect theoretical tools to be free of such challenges, but this is not the case. Indeed, theoretically, first-principles calculations and symmetry analysis are employed to identify the space group of materials, but these methods are also subject to limitations.

A first limitation comes from the finite precision of first-principles calculations. In order to mitigate such finite precision, the symmetry analysis must incorporate a tolerance. However, for a given set of atomic positions (with possible uncertainty), one might get different space groups for the system by playing with the tolerance for the symmetry recognition. Ignoring the decimal digits for the atomic position beyond some predetermined tolerance while using the higher value of tolerance for the symmetry might make the system more symmetric than it is, hence a higher space group would be assigned to the system. However, it is well documented that there are many cases of spontaneous symmetry breaking, so not all materials prefer to be in a higher symmetric state, and some systems [46] prefer to remain in a lower symmetric state as well. Hence, matching the finite precision of the first-principles calculation with the tolerance for symmetry is an important source of potential problems.

A second caveat comes as a side effect of the users' desire to spare computing time. Use of symmetries is a powerful tool to streamline such calculations. Hence, the symmetries detected from the input file are usually frozen in, and never questioned again during or after the first-principles geometry optimization. At least a local stability analysis should be done, e.g., checking with a phonon band structure calculation that there is no spontaneous second-order phase transition. But also, the symmetry assignment should be reexamined after first-principles optimization, while this is not the case in most well-known packages. Thus, in addition to the aforementioned tolerance issue, the symmetry analysis of the first-principles geometry refinement result is bypassed, and lastly, no stability check is carried out.

In order to obtain a sufficiently precise atomic position and, hence, accurately establish the space group of the system, one must reduce the tolerance value over the forces required for the system relaxation, provided that the tolerance value for symmetry recognition is sufficiently minimal.

To add more confusion to this challenge, different DFT codes might use different values for these tolerances to determine the ground state of the materials. Minor variations in the tolerance for symmetry or the tolerance over the maximum forces can lead to different space group identification, as we shall demonstrate.

As a final warning, it has been reported before [47] that the sole determination of the space group for a fixed geometry by different packages, namely FINDSYM [48], PLATON [49], Spglib [50,51], or AFLOW-SYM [47] might deliver different results, even with human-tuned tolerances. It is unclear what is the cause of such failures, and bugs in the implementation cannot be excluded.

III. NUMERICAL METHODOLOGY

The first-principles calculations we present in this work were performed using the ABINIT [52–54] (version 9.11.6.1) software package with norm-conserving scalar relativistic pseudopotentials [55] from the PSEUDO-DOJO project [56] (version 0.5) and the GGA-PBE [57,58] exchange-correlation functional. Since both the MC2D and C2DB databases use the GGA-PBE exchange-correlation functional, it is the most logical choice for investigating space group assignments from our first-principles calculations. To ensure consistency across all calculations, a standardized approach to Brillouin zone sampling is adopted for all systems. The converged planewave kinetic energy energy cut-off is 50 Ha (about 1361 eV). A 8x8x1 electronic wavevector grid for Brillouin zone sampling is used for the study of all materials. For the treatment of metals, the C2DB database uses 0.05 eV smearing. We have tested different smearing for ABINIT, without significant effect on space group recognition. For the CrS_2 results shown later, a smearing of 0.02 Ha (about 0.5 eV) was used. The phonons were computed using density-functional perturbation theory (DFPT) [59–62] implemented inside ABINIT and the phonon dispersions are plotted using AbiPy Python scripts.

As mentioned in the previous section, one needs to define the tolerance for the determination of the space group and the tolerance for the determination of the optimized geometry. In ABINIT, the tolerance for the determination of space group and the tolerance for forces are named `tolsym` and `tolmxf`, respectively. ABINIT uses the default values of 10^{-5} for `tolsym` (reduced coordinates for atomic positions, and relative values for lattice vectors) and 5×10^{-5} Ha/Bohr (2.57 meV/Å) for `tolmxf`.

The MC2D database creates the 2D materials by exfoliating experimental bulk (3D) materials extracted from the Inorganic Crystal Structure Database (ICSD) [63], the Crystallography Open Database (COD) [64], and the Materials Platform for Data Science (MPDS) [65] databases. In the same spirit, the C2DB database uses the ICSD, COD, Open Quantum Materials Database (OQMD) [66], and Materials Project (MP) databases to exfoliate 2D materials from its bulk parent structures.

In the MC2D database, the structural relaxation is done through the Quantum ESPRESSO [67] code with DFT-PBE van der Waals functionals [68] and pseudopotentials from the standard solid-state pseudopotentials (SSSP) library [69]. The C2DB database performs structural relaxations using the GPAW [70] code, which employs projector augmented wave (PAW) [71] potentials and planewave basis sets. The C2DB calculations also utilize the PBE exchange-correlation functional for structure and energetics.

The force tolerance used during the structural relaxations of the MC2D database is not explicitly reported in its publication [11]. However, the Quantum ESPRESSO code uses default values of 10^{-5} for tolerance for symmetry and 10^{-3} Ha/Bohr (51.4 meV/Å) for tolerance over forces, defining the convergence criterion during atomic relaxation. The C2DB uses 10^{-4} for tolerance for symmetry and 10 meV/Å for tolerance over the forces for the structural relaxation (the same as ABINIT).

TABLE I. For each of the materials, space group obtained when starting either from the MC2D database or from the C2DB database. The "Database" column indicates the space group mentioned in the database. The "Unrelaxed" and "Relaxed" columns, respectively, mention the space groups recognized by ABINIT before relaxation (i.e., taking the structure from the database without modification) and after relaxation with a stringent value of `tolmxf`, respectively. No stability analysis is done after relaxation. Three sets of materials emerge; see text. In the set-3, the phases with space groups mentioned between parentheses were not present in C2DB at the start of our investigation, in 2023.

		MC2D			C2DB		
			ABINIT			ABINIT	
Sets	Materials	Database	Unrelaxed	Relaxed	Database	Unrelaxed	Relaxed
	CrI_3	$P\bar{3}$	$P\bar{3}$	$P\bar{3}1m$	$P\bar{3}1m$	$P\bar{3}1m$	$P\bar{3}1m$
	$CrBr_3$	$P\bar{3}$	$P\bar{3}$	$P\bar{3}1m$	$P\bar{3}1m$	$P\bar{3}1m$	$P\bar{3}1m$
	$CrGeTe_3$	$P\bar{3}$	$P\bar{3}$	$P\bar{3}1m$	$P\bar{3}1m$	$P\bar{1}$	$P\bar{3}1m$
	$CrSiSe_3$	$P\bar{3}$	$P\bar{3}$	$P\bar{3}1m$	$P\bar{3}1m$	$P\bar{3}1m$	$P\bar{3}1m$
set-1	$CrSiTe_3$	$P\bar{3}$	$P\bar{3}$	$P\bar{3}1m$	$P\bar{3}1m$	$P\bar{3}1m$	$P\bar{3}1m$
	$MnPS_3$	$P\bar{1}$	$P\bar{1}$	$P\bar{3}1m$	$P\bar{3}1m$	$P\bar{3}1m$	$P\bar{3}1m$
	$MnPSe_3$	$P\bar{3}$	$P\bar{3}$	$P\bar{3}1m$	$P\bar{3}1m$	$P\bar{3}1m$	$P\bar{3}1m$
	$NiPS_3$	Cm	C2/m	$P\bar{3}1m$	$P\bar{3}1m$	$P\bar{3}1m$	$P\bar{3}1m$
	$NiPSe_3$	Cm	C2/m	$P\bar{3}1m$	$P\bar{3}1m$	$P\bar{3}1m$	$P\bar{3}1m$
set-2	$CrCl_3$	C2	C2/m	C2/m	$P\bar{3}1m$	$P\bar{3}1m$	$P\bar{3}1m$
	CrS_2	P3m1	$P\bar{3}m1$	$P\bar{3}m1$	$P\bar{6}m2$ ($P\bar{3}m1$)	$P\bar{6}m2$ ($P\bar{3}m1$)	$P\bar{6}m2$ ($P\bar{3}m1$)
	$CrTe_2$	$P\bar{3}m1$	$P\bar{3}m1$	$P\bar{3}m1$	$P\bar{6}m2$ ($P\bar{3}m1$)	$P\bar{6}m2$ ($P\bar{3}m1$)	$P\bar{6}m2$ ($P\bar{3}m1$)
set-3	VS_2	$P\bar{3}m1$	$P\bar{3}m1$	$P\bar{3}m1$	$P\bar{6}m2$ ($P\bar{3}m1$)	$P\bar{6}m2$ ($P\bar{3}m1$)	$P\bar{6}m2$ ($P\bar{3}m1$)
	VSe_2	$P\bar{3}m1$	$P\bar{3}m1$	$P\bar{3}m1$	$P\bar{6}m2$ ($P\bar{3}m1$)	$P\bar{6}m2$ ($P\bar{3}m1$)	$P\bar{6}m2$ ($P\bar{3}m1$)
	VTe_2	$P\bar{3}m1$	$P\bar{3}m1$	$P\bar{3}m1$	$P\bar{6}m2$ ($P\bar{3}m1$)	$P\bar{6}m2$ ($P\bar{3}m1$)	$P\bar{6}m2$ ($P\bar{3}m1$)

The C2DB database uses a vacuum spacing between the slabs of 15 Å for isolated 2D units during structural relaxation, while the MC2D database employs a larger vacuum spacing of 20 Å. After perfororming a convergence study for ML CrI_3, we choose a vacuum spacing close to 15 Å for our studies, which is sufficient for our desired accuracy.

IV. RESULTS AND DISCUSSION

In the process of finding the real ground-state space group of the materials, in 2023, we found that at least fifteen materials were reported with different space groups in different databases. After analyzing the origin of the disparity, we classified them in three sets as reported in Table I.

The materials in the first set are such that the higher symmetry space group is the correct one, and this higher symmetry space group contains all the symmetries of the lower symmetry space group. For one specific material, the lower symmetry space group is the correct one, and the structure with the higher symmetry space group is not energetically favored. This material, $CrCl_3$, is categorized in set-2. In the third set, materials with the same stoichiometry but different bonding topologies (so, different phases) were present in these two databases in 2023. In the latter case, going from one bonding topology to the other requires a distortion that breaks both space groups. However, during the time of our study, the C2DB database was enlarged, and structures similar to those of the MC2D were added, reducing the mismatch between the two databases.

Note that, in comparing different databases, we filter only phases that are reported to have the same stoichiometry and the same number of atoms per unit cell.

MC2D database does not test the magnetic ordering of these reported materials except some materials from set-3 materials. In contrast, the C2DB database tests the magnetic ordering of most of these materials. For all materials reported, the first-principles study is restricted to collinear magnetic ordering.

At the end of this section, we also propose a protocol to unravel the space group confusion. Additional information on cell parameters and atomic coordinates is provided in the Supplemental Material [73]. These are used to produce the figures reported in the current publication.

For a better understanding of the results, the relevant group-subgroup relations are reported in Fig. 1. The space groups lying in one cascade (i.e., $P\bar{3}1m$ - $P\bar{3}$ - $P\bar{1}$, $P\bar{3}1m$ - C2/m - C2 and $P\bar{3}1m$ - C2/m - Cm) are related by small symmetry-breaking distortions. P3m1 is the subgroup of both $P\bar{3}m1$ and $P\bar{6}m2$ space groups whereas $P\bar{3}m1$ and $P\bar{6}m2$ are not directly related by any relations.

A. Set-1

After structural relaxation with ABINIT for all the set-1 materials with the above-mentioned parameter settings, and

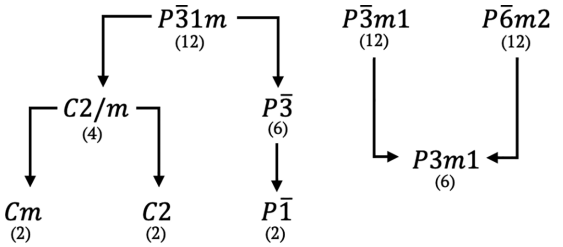

FIG. 1. Group-subgroup trees that show the relationship between different space groups. Arrow head is always pointing towards the subgroups whereas nock of the arrow is the supergroup. The numbers in the bracket, lying below each space group show the number of different translational classes of symmetries in that particular space group.

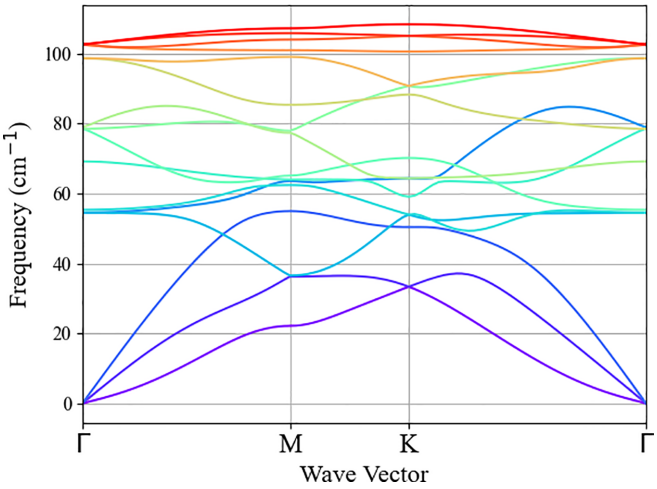

FIG. 2. Phonon dispersion curves of the ferromagnetic monolayer CrI_3 in its space group P$\bar{3}$1m.

a stringent value for `tolmxf` of 10^{-8} Ha/Bohr (about 5×10^{-4} meV/Å) along with the default value of `tolsym`, the higher symmetry structure, i.e., P$\bar{3}$1m is found, irrespective of the initial structure from MC2D or C2DB. We describe now the case of ML CrI_3 in detail. As mentioned in the introduction, for this material, additional starting points and space groups exist in the literature.

In Table II, we report the total energies obtained before and after the structural relaxation of the ML CrI_3 performed using the above-mentioned parameters and tolerances for both ferromagnetic and antiferromagnetic ordering. The structure with C2 and C2/m space groups are generated by cleaving layer from their bulk parent reported in Materials Project [72] database. The other structure with P$\bar{3}$ and P$\bar{3}$1m space group are taken from the MC2D and C2DB database. All the initial structures with different space groups relax to the same structure, recognized to be one of the higher symmetry space groups, i.e., P$\bar{3}$1m, preferring ferromagnetic ordering. The energy difference between the final structures is less than 0.01 meV. The absolute total energy per atom of the reference (lowest energy) structure is $E = -869999.88$ meV/atom.

In line with the difficulties mentioned earlier, we also computed the phonon band structure of ML CrI_3 with P$\bar{3}$m1 space group and the lowest energy that we obtained after structural relaxation, to ensure it is at least a locally stable phase. The phonon band structure is shown in Fig. 2. No instability is present, confirming that the structure with P$\bar{3}$m1 space group is the lowest energy state for ML CrI_3 among all locally distorted structures.

We also tried to understand the wrong assessment of the space group of ML CrI_3 by different sources. In order to shed light on this problem, we performed such assessment for a range of `tolsym` values, including extremely loose ones, and, in the relaxed situation, for a range of `tolmxf` values including extremely loose ones. The results are shown in Fig. 3 that can be seen as a kind of "phase diagram". The P$\bar{3}$1m region in the phase diagram is present for both MC2D and C2DB initial structures, but only for a relatively loose value of `tolsym` in the case of the MC2D database. This starting point is thus relatively inaccurate. In the case of the ABINIT relaxation, the P$\bar{3}$1m region gets more extended when more stringent values of `tolmxf` ($\leqslant 10^{-8}$ Ha/Bohr) are used. In contrast, when `tolmxf` is loose, the C2 space group is favored. A very loose value of `tolsym` can also give the right P$\bar{3}$1m space group.

In a small region in this phase diagram, C2/m is the identified space group. We note that the slope of `tolmxf` versus `tolsym` defining the boundaries of this region with both the C2 and the P$\bar{3}$1m regions is approximately linear. So, for this example, `tolmxf`, expressed in Ha/Bohr, must be approximately hundred times smaller than `tolsym` (or even lower) to stay in the P$\bar{3}$1m region.

TABLE II. Comparison of the energies and space groups of monolayer CrI_3 before ("Unrelaxed" columns) and after ("Relaxed" columns) ABINIT relaxation in both antiferromagnetic (AFM) and ferromagnetic (FM) states, the lowest energy phase being taken as the zero reference. Structures with energy difference less than 0.01 meV/atom are quite similar and are recognized by ABINIT to belong to the same space group, with the default ABINIT value of `tolsym`, 10^{-5}.

Initial space group	Difference in total energy ΔE (meV/atom)				Final space group
	AFM		FM		
	Unrelaxed	Relaxed	Unrelaxed	Relaxed	(both FM and AFM)
C2 [72]	5.587	4.492	0.685	0.008	P$\bar{3}$1m
C2/m [13]	4.730	4.488	0.193	0.002	P$\bar{3}$1m
P$\bar{3}$ [11]	20.865	4.489	18.445	0.003	P$\bar{3}$1m
P$\bar{3}$1m [12,14]	4.758	4.489	0.040	0.000	P$\bar{3}$1m

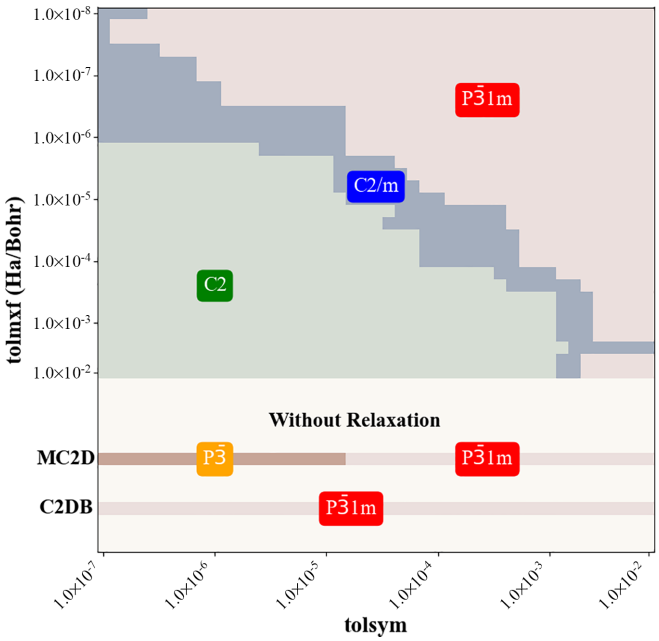

FIG. 3. Space group "phase diagram" for ferromagnetic monolayer CrI_3. Regions for C2, C2/m, P$\bar{3}$, and P$\bar{3}$1m space groups are presented with green, blue, orange, and red colors respectively. (Lower panel) The structure is taken straight from MC2D and C2DB database, and the space group is shown as a function of `tolmxf`. (Upper panel) The structure is relaxed using `tolmxf` as stopping criterion for ABINIT, and the space group is recognized using `tolsym` as tolerance.

Using a loose `tolsym` is of course not a correct strategy, since it will favor the higher symmetry space group, while there are cases in which the lower space group is favored, as will be the case for the materials in the second set.

B. Set-2

The second set is for materials in which the different structures are related by group-subgroup relation as in the case of set-1 materials. However, the lower-symmetry space group structures are energetically favored. ML $CrCl_3$ belongs to this case.

The space group of ML $CrCl_3$ is reported to be C2 in the MC2D database. ABINIT recognizes its space group to be C2/m with the default value of `tolsym`. However, this value is similar to the default value of Quantum ESPRESSO used for MC2D. We assume that the space group C2 is reported incorrectly or that MC2D is using a lower tolerance value for the space-group recognition.

Anyhow, after aligning the structures taken from MC2D and C2DB for comparison, we observed that the lower symmetry structure, i.e., C2/m, is more stable than the higher symmetry one, unlike for set-1 materials. We then computed the total energy along a path connecting the two structures. The result is shown in the energy landscape in Fig. 4. The total energy of the P$\bar{3}$1m structure is not the lowest value. The total energy starting from the P$\bar{3}$1m structure is lowered along this path. The energy minimum is located close to, but not exactly at, the optimized C2/m structure. This small difference is a

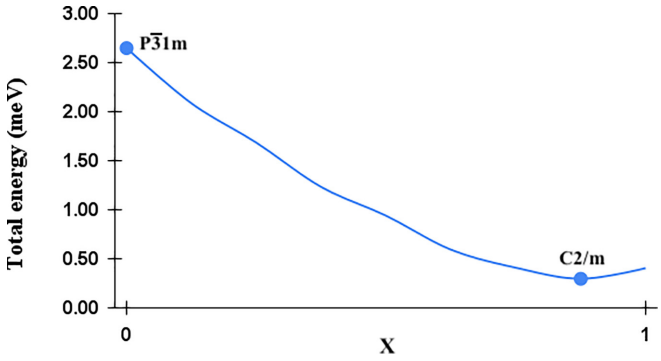

FIG. 4. The total energy of ML $CrCl_3$ (3 atoms/cell) along a linear path connecting the P$\bar{3}$1m structure ($x = 0$) to the lowest energy C2/m structure ($x = 1$) obtained after relaxation (atomic positions and lattice parameters) with the stringent value of `tolmxf`.

side effect of stopping the relaxation for some finite value of `tolmxf`, also at an energy level where eggbox effects [74,75] with the exchange-correlation energy treatment using a grid in real space start to contaminate the otherwise smooth behavior of the energy as a function of the atomic coordinates and lattice parameters.

This example demonstrates that setting `tolsym` to a loose level can fail to determine the correct space group of the material. In Table I, it is shown that for this material ABINIT correctly finds the space group starting from the lower-symmetry structure delivered by the MC2D database, while it stays in the incorrect high-symmetry space group when considering the C2DB structure as input.

C. Set-3

When we started this investigation in 2023, most of the set-3 materials were reported with P$\bar{3}$m1 and P$\bar{6}$m2 space groups, in MC2D and C2DB databases, respectively, as shown in Table I. Only CrS_2 was reported with the P3m1 space group in 3 atom unit cell, from MC2D. However, since then, C2DB has been enlarged. It now reports the set-3 materials in different phases, including some with more number of atoms in the unit cell than the ones originally listed. We report in Table I only the structures with the same number of atoms in the unit cell from both databases in order to maintain consistency.

In reference to the situation presented in 2023, the confusion for these materials arose because the two databases listed different polymorphs with the same composition and stoichiometry. These polymorphs have a different bonding topology, unlike set-1 and set-2 materials. Even after structural relaxation with stringent tolerance values, the set-3 materials retain the P$\bar{3}$m1 (even for CrS_2) and P$\bar{6}$m2 space group structures taken from MC2D and C2DB respectively. Going from one polymorph to the other involves breaking bonds, and there is an energy barrier along the connecting path.

CrS_2 is taken as an illustrative example. From our study, the P$\bar{3}$m1 space group structure is a ferromagnetic metal, while the P$\bar{6}$m2 space group structure, with a lower energy, is a nonmagnetic gapped material. The C2DB database reports

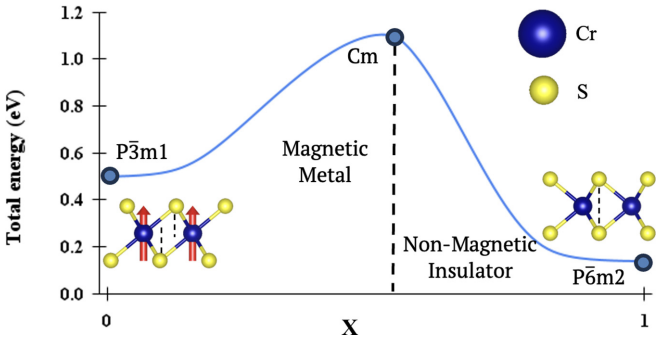

FIG. 5. Total energy of monolayer CrS_2 (3 atoms/cell) along the path going from the P$\bar{3}$m1 space group structure (magnetic) to the P$\bar{6}$m2 space group structure (nonmagnetic). The dot close to the top of the vertical-dotted line presents the point of transition from magnetic to nonmagnetic ordering whereas the dots at both ends of the curve present the initial and final space groups of the material.

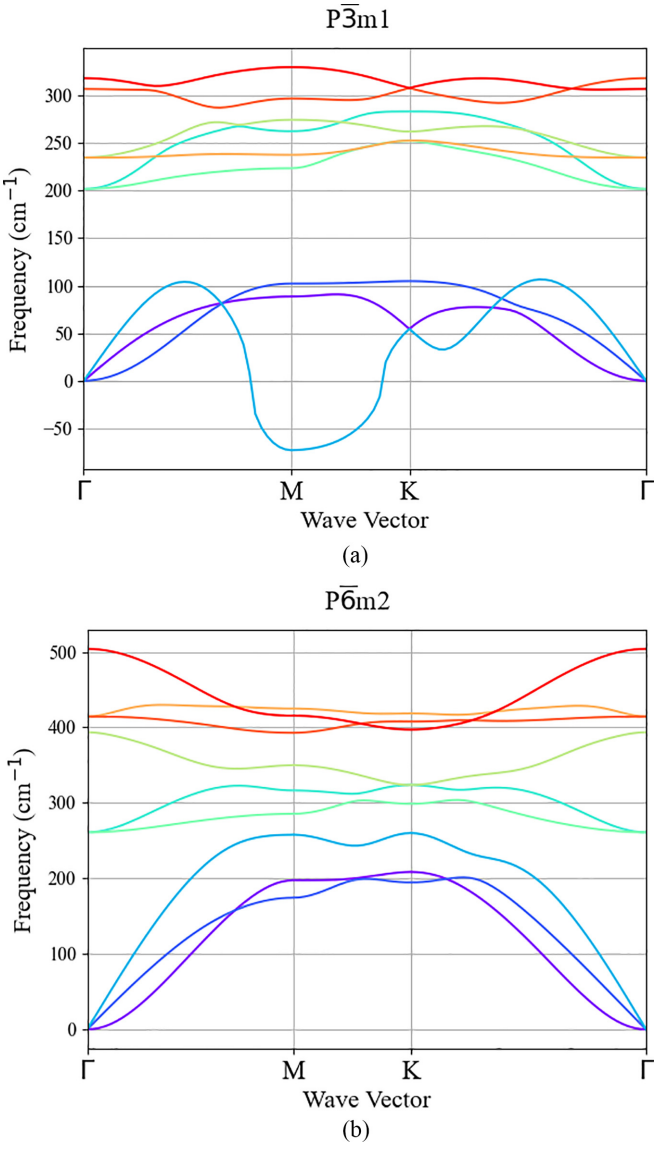

FIG. 6. Monolayer CrS_2 phonon band structures for (a) the P$\bar{3}$m1 polymorph and (b) the P$\bar{6}$m2 polymorph, both with 3 atoms per cell. In (a), the imaginary frequencies are shown as negative.

that all structures of CrS_2 are nonmagnetic, while the MC2D does not report the magnetic ordering.

The result of a nudged elastic band (NEB) [76–79] study is shown in Fig. 5. The space group of the structures lying on the line connecting the P$\bar{3}$m1 to P$\bar{6}$m2 space group structures is Cm. To transform the structure from P$\bar{3}$m1 to P$\bar{6}$m2 space group, not only bonds are broken but magnetic ordering also changes. The energy barrier is about 1 eV above the energy of the P$\bar{6}$m2 space group structure. The switch from magnetic to non-magnetic ordering occurs close, but not exactly at, the maximum of energy (dashed-vertical line in Fig. 5).

Although one might be satisfied with such a result, the determination of the ground-state structure might still be incorrect, if one or the other phase spontaneously distorts. This is precisely the case of the structure with P$\bar{3}$m1 space group. The phonon band structures of both P$\bar{3}$m1 and P$\bar{6}$m2 polymorphs are shown in Fig. 6. For the P$\bar{3}$m1 polymorph, the presence of imaginary frequencies (shown as negative in the vertical axis) is observed in a large neighborhood around the M (1/2, 0, 0) wavevector. Thus, this P$\bar{3}$m1 phase is not even metastable, unlike the P$\bar{6}$m2 phase. By freezing a finite collective displacement with the eigenvector of the unstable phonon mode at M (1/2, 0, 0) [61,80–83], so doubling the size of the initial primitive cell, then relaxing the structure, a lowering of total energy of 0.37 eV is observed. A stable phase with $P2_1/m$ space group is obtained. Like the unstable P$\bar{3}$m1 phase, it is also a ferromagnetic metal. In a final step, the stability of this $P2_1/m$ structure is verified by computing its phonon band structure, see Fig. 7. All phonon modes are stable. Hence, we can conclude that this is the correct locally stable structure with this bonding topology, unlike the one presented in the C2DB database.

Similarly, monolayer $CrTe_2$ and VTe_2 also exhibit unstable phonons at finite momentum in the P$\bar{3}$m1 phase whereas VS_2 and VTe_2 are stable in both P$\bar{3}$m1 and P$\bar{6}$m2 phases. Finally, monolayer $CrTe_2$ shows the same kind of magnetic and nonmagnetic behavior in different phases as monolayer CrS_2.

This unstable P$\bar{3}$1m structure, and the final stability of the $P2_1/m$ establishes that one cannot rely on the structure of the materials reported in the databases if their stability has not been checked with a local stability analysis thanks to a phonon band structure. Additionally, the scenario found in the set-3 materials is a warning that 2D materials might be present in distinct polymorphs. The careless joint exploitation of different databases may lead to inconsistent or inaccurate findings. Additionally, the tensorial characteristics [35] of materials that are sensitive to space groups, such as flexoelectricity, magnetoelectricity, and altermagnetism could potentially be predicted wrongly.

As an additional example, in a recent publication [39], authors attempt to find possible 2D altermagnets on the basis of their space group symmetry, from the list of materials reported in the C2DB database through high throughput calculations. However, we found at least three materials (i.e., RuF_4, VF_4, and $FeBr_3$) from the list of seven materials mentioned in the publication, to be reported with different space groups in both the MC2D and C2DB databases.

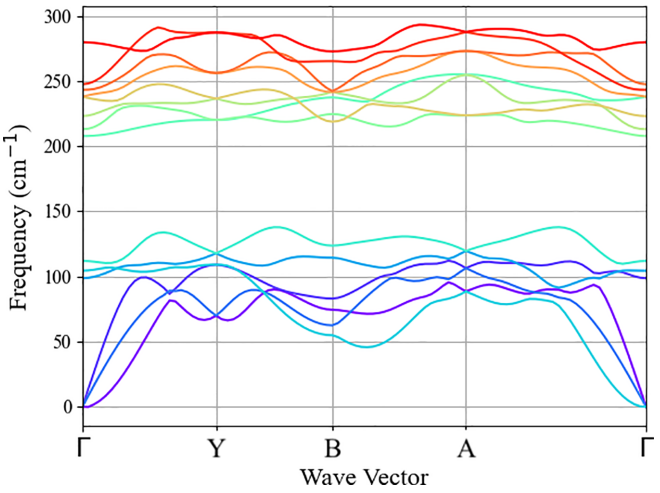

FIG. 7. Monolayer CrS_2 phonon band structure for the structure with $P2_1/m$ space group (6 atoms per cell), around the high-symmetry points Γ (0,0), Y (0,1/2), B (1/2,0), and A (1/2,1/2).

D. A protocol to better determine the space group

Having identified different sources of confusion, one can wonder whether there is a fool-proof recipe to determine the space group of materials in databases. From the very start, since one has to play with tolerances, there might always be exceptions that fall below the tolerance. Thus, one can never be sure that the determination has been achieved with absolute certainty. Still, a protocol to better handle this problem can be proposed, on the basis of the present study. All the materials presented in this publication have been studied using this protocol.

First, for each single starting structure, one has to improve the confidence that this is a locally stable structure, with a correctly identified space group for a given, sufficiently stringent value of `tolsym`. This is achieved by:

(1.A) A first determination of the space group of the starting structure.

(1.B) Relaxation of the structure using a value of `tolmxf` that is tuned to the value of `tolsym`. In this respect, the default value of `tolmxf` for ABINIT was found to be too loose, i.e., `tolmxf` $= 10^{-8}$ Ha/Bohr (about 5×10^{-4} meV/Å) was needed to ensure a numerically accurate optimized geometry.

(1.C) Redetermination of the space group. If the space group changed, possible further study of the effect of both `tolsym` and `tolmxf` may be needed.

(1.D) Check that the structure is locally stable, thanks to a phonon band structure calculation.

(1.E) For the structure with any instability, a finite collective displacement with the eigenvector of the detected unstable phonon is frozen, then the structure is re-optimized, to obtain the truly stable phase of the material, following again the previous steps.

Second, if more than one space group stems from such an analysis, one has to suspect that the system has more than one polymorph, and thus, one should:

(2.A) Examine the group-subgroup relationship between the different optimized structures.

(2.B) Study materials with different space groups with NEB calculations to see the presence of a real energy barrier or any spontaneous symmetry breaking.

V. CONCLUSIONS

In this work, we addressed the challenge of determining the true ground-state space group of monolayer CrI_3 and other 2D materials, which have been inconsistently classified across various publications and databases. Monolayer CrI_3 is particularly intriguing, since it has been reported with four different space groups, reflecting a significant ambiguity in the literature. To resolve this uncertainty, we propose a protocol that combines density functional theory calculations, symmetry analysis, phonon band structure calculations, and energy minimization, in order to more reliably determine the real ground state of such materials, with no absolute certainty, however.

By applying this protocol, we find that the ground-state space group of ML CrI_3 is $P\bar{3}1m$, providing a definitive resolution to the disparities reported previously. Extending our analysis to fourteen other 2D materials with conflicting space group assignments, we classified these materials into three distinct sets based on their ground-state symmetry behavior. The first set comprises materials whose ground state corresponds to a higher-symmetry structure, consistent with most initial reports. The second set includes materials where the ground state exhibits a lower-symmetry space group, underscoring the limitations of relying solely on database-reported structures. The third set involves materials exhibiting polymorphism, with two distinct and energetically stable configurations corresponding to different space groups. This dual stability highlights an intriguing interplay between energy minima and suggests potential avenues for exploring functional tunability through external factors such as strain or temperature.

Moreover, in this third set, we have examined in detail the case of CrS_2, where the $P\bar{3}1m$ polymorph listed in the MC2D and C2DB is not stable, but spontaneously distorts to a structure with $P2_1/m$ space group. We have checked the stability of the latter thanks to its phonon band structure.

Our findings not only resolve ambiguities in the reported structures of these materials but also demonstrate the necessity of systematic protocols for accurate space group classification. The observed polymorphism and variations in ground-state symmetry reveal a rich landscape of structural possibilities in 2D materials, providing insights into their underlying physics and potential applications. This work establishes a robust framework for addressing similar inconsistencies in other materials, and serves as a benchmark for reliable structural determination in the rapidly evolving field of 2D materials.

ACKNOWLEDGMENTS

This work is an outcome of the Shapeable 2D magneto-electronics by design project (SHAPEme, EOS Project No. 560400077525) that has received funding from the FWO and FRS-FNRS under the Belgian Excellence of Science (EOS) program. Computational resources have been provided by the

supercomputer facility of the Consortium des Équipements de Calcul Intensif (CECI) funded by the FRS-FNRS under Grant No. 2.5020.11.

DATA AVAILABILITY

The data supporting this study's findings are available within the article.

[1] K. S. Novoselov, A. K. Geim, S. V. Morozov, D. Jiang, Y. Zhang, S. V. Dubonos, I. V. Grigorieva, and A. A. Firsov, Science **306**, 666 (2004).

[2] M. Sang, J. Shin, K. Kim, and K. J. Yu, Nanomaterials **9**, 374 (2019).

[3] J. D. Renteria, D. L. Nika, and A. A. Balandin, Appl. Sci. **4**, 525 (2014).

[4] R. Mas-Balleste, C. Gomez-Navarro, J. Gomez-Herrero, and F. Zamora, Nanoscale **3**, 20 (2011).

[5] M. M. Uddin, M. H. Kabir, M. A. Ali, M. M. Hossain, M. U. Khandaker, S. Mandal, A. Arifutzzaman, and D. Jana, RSC Adv. **13**, 33336 (2023).

[6] N. D. Mermin and H. Wagner, Phys. Rev. Lett. **17**, 1133 (1966).

[7] B. Huang, G. Clark, E. Navarro-Moratalla, D. R. Klein, R. Cheng, K. L. Seyler, D. Zhong, E. Schmidgall, M. A. McGuire, D. H. Cobden *et al.*, Nature (London) **546**, 270 (2017).

[8] Y. Zhao, L. Lin, Q. Zhou, Y. Li, S. Yuan, Q. Chen, S. Dong, and J. Wang, Nano Lett. **18**, 2943 (2018).

[9] C. Gong and X. Zhang, Science **363**, eaav4450 (2019).

[10] Y. Zhumagulov, S. Chiavazzo, I. A. Shelykh, and O. Kyriienko, Phys. Rev. B **108**, L161402 (2023).

[11] D. Campi, N. Mounet, M. Gibertini, G. Pizzi, and N. Marzari, "The Materials Cloud 2D database (MC2D)", Materials Cloud Archive (2022), https://doi.org/10.24435/materialscloud:36-nd.

[12] S. Haastrup, M. Strange, M. Pandey, T. Deilmann, P. S. Schmidt, N. F. Hinsche, M. N. Gjerding, D. Torelli, P. M. Larsen, A. C. Riis-Jensen *et al.*, 2D Mater. **5**, 042002 (2018).

[13] L. Webster, L. Liang, and J.-A. Yan, Phys. Chem. Chem. Phys. **20**, 23546 (2018).

[14] C. Bacaksiz, D. Šabani, R. M. Menezes, and M. V. Milošević, Phys. Rev. B **103**, 125418 (2021).

[15] M. Och, M.-B. Martin, B. Dlubak, P. Seneor, and C. Mattevi, Nanoscale **13**, 2157 (2021).

[16] J.-Y. You, Z. Zhang, X.-J. Dong, B. Gu, and G. Su, Phys. Rev. Res. **2**, 013002 (2020).

[17] F. Han, X. Yan, A. Bergara, W. Li, H. Yu, and G. Yang, Phys. Chem. Chem. Phys. **25**, 29672 (2023).

[18] X. Wang, X.-P. Li, J. Li, C. Xie, J. Wang, H. Yuan, W. Wang, Z. Cheng, Z.-M. Yu, and G. Zhang, Adv. Funct. Mater. **33**, 2304499 (2023).

[19] S. N. Neal, H.-S. Kim, K. A. Smith, A. V. Haglund, D. G. Mandrus, H. A. Bechtel, G. L. Carr, K. Haule, D. Vanderbilt, and J. L. Musfeldt, Phys. Rev. B **100**, 075428 (2019).

[20] J. Yang, Y. Zhou, Q. Guo, Y. Dedkov, and E. Voloshina, RSC Adv. **10**, 851 (2020).

[21] M. Mi, X. Zheng, S. Wang, Y. Zhou, L. Yu, H. Xiao, H. Song, B. Shen, F. Li, L. Bai *et al.*, Adv. Funct. Mater. **32**, 2112750 (2022).

[22] P. Li, X. Li, J. Feng, J. Ni, Z.-X. Guo, and H. Xiang, Phys. Rev. B **109**, 214418 (2024).

[23] A. Musari and P. Kratzer, Mater. Res. Express **9**, 106302 (2022).

[24] T. Y. Kim and C.-H. Park, Nano Lett. **21**, 10114 (2021).

[25] M. Wu, Z. Li, and S. G. Louie, Phys. Rev. Mater. **6**, 014008 (2022).

[26] K. Kim, S. Y. Lim, J.-U. Lee, S. Lee, T. Y. Kim, K. Park, G. S. Jeon, C.-H. Park, J.-G. Park, and H. Cheong, Nat. Commun. **10**, 345 (2019).

[27] M. A. McGuire, G. Clark, S. Kc, W. M. Chance, G. E. Jellison, Jr., V. R. Cooper, X. Xu, and B. C. Sales, Phys. Rev. Mater. **1**, 014001 (2017).

[28] K. Chen, J. Deng, Y. Yan, Q. Shi, T. Chang, X. Ding, J. Sun, S. Yang, and J. Z. Liu, npj Comput. Mater. **7**, 79 (2021).

[29] Q. Wei, D. Chen, C. Yongqing, S. Lei, X. Jing, Y. Jiaren, C. Yuanping, and Y. Xiaohong, J. Supercond. Novel Magn. **35**, 787 (2022).

[30] Y. Liu, S. Kwon, G. J. de Coster, R. K. Lake, and M. R. Neupane, Phys. Rev. Mater. **6**, 084004 (2022).

[31] J.-J. Xian, C. Wang, J.-H. Nie, R. Li, M. Han, J. Lin, W.-H. Zhang, Z.-Y. Liu, Z.-M. Zhang, M.-P. Miao *et al.*, Nat. Commun. **13**, 257 (2022).

[32] E. B. Isaacs and C. A. Marianetti, Phys. Rev. B **94**, 035120 (2016).

[33] H. Sheng, H. Long, G. Zou, D. Bai, J. Zhang, and J. Wang, J. Mater. Sci. **56**, 15844 (2021).

[34] G. Miao, S. Xue, B. Li, Z. Lin, B. Liu, X. Zhu, W. Wang, and J. Guo, Phys. Rev. B **101**, 035407 (2020).

[35] E. Kroumova, M. I. Aroyo, J. M. Perez-Mato, A. Kirov, C. Capillas, S. Ivantchev, and H. Wondratschek, Phase Transitions **76**, 155 (2003).

[36] M. Kruse, U. Petralanda, M. N. Gjerding, K. W. Jacobsen, K. S. Thygesen, and T. Olsen, npj Comput. Mater. **9**, 45 (2023).

[37] Z.-F. Gao, S. Qu, B. Zeng, Y. Liu, J.-R. Wen, H. Sun, P.-J. Guo, and Z.-Y. Lu, Natl. Sci. Rev. **12**, nwaf066 (2025).

[38] S. Zeng and Y.-J. Zhao, Phys. Rev. B **110**, 054406 (2024).

[39] J. Sødequist and T. Olsen, Appl. Phys. Lett. **124**, 182409 (2024).

[40] C. Xin, B. Song, G. Jin, Y. Song, and F. Pan, Adv. Theor. Simul. **6**, 2300475 (2023).

[41] G. R. Schleder, B. Focassio, and A. Fazzio, Appl. Phys. Rev. **8**, 031409 (2021).

[42] K. Wagoner-Oshima, R. Bhattarai, H. Terrones, and T. D. Rhone, ACS Appl. Mater. Interfaces **17**, 11002 (2025).

[43] T. H. B. da Silva, T. Cavignac, T. F. T. Cerqueira, H.-C. Wang, and M. A. L. Marques, Mater. Horiz. **12**, 3408 (2025).

[44] D. Pant, H. B. Tripathi, and D. D. Pant, J. Lumin. **51**, 223 (1992).

[45] J. Gates, A. Atrens, and I. Smith, Mater. Werkstofftech. **18**, 179 (1987).

[46] C. Cazorla and T. Gould, Sci. Adv. **5**, eaau5832 (2019).

[47] D. Hicks, C. Oses, E. Gossett, G. Gomez, R. H. Taylor, C. Toher, M. J. Mehl, O. Levy, and S. Curtarolo, Acta Crystallogr., Sect. A: Found. Adv. **74**, 184 (2018).

[48] H. T. Stokes and D. M. Hatch, J. Appl. Crystallogr. **38**, 237 (2005).

[49] A. L. Spek, Acta Crystallogr., Sect. D: Biol. Crystallogr. **65**, 148 (2009).

[50] A. Togo, K. Shinohara, and I. Tanaka, Sci. Technol. Adv. Mater., Meth. **4**, 2384822 (2024).

[51] K. Shinohara, A. Togo, and I. Tanaka, Acta Crystallogr. Sect. A: Found. Adv. **79**, 390 (2023).

[52] X. Gonze, B. Amadon, G. Antonius, F. Arnardi, L. Baguet, J.-M. Beuken, J. Bieder, F. Bottin, J. Bouchet, E. Bousquet *et al.*, Comput. Phys. Commun. **248**, 107042 (2020).

[53] X. Gonze, J.-M. Beuken, R. Caracas, F. Detraux, M. Fuchs, G.-M. Rignanese, L. Sindic, M. Verstraete, G. Zerah, F. Jollet *et al.*, Comput. Mater. Sci. **25**, 478 (2002).

[54] A. H. Romero, D. C. Allan, B. Amadon, G. Antonius, T. Applencourt, L. Baguet, J. Bieder, F. Bottin, J. Bouchet, E. Bousquet *et al.*, J. Chem. Phys. **152**, 124102 (2020).

[55] D. R. Hamann, Phys. Rev. B **95**, 239906(E) (2017).

[56] M. J. V. Setten, M. Giantomassi, E. Bousquet, M. J. Verstraete, D. R. Hamann, X. Gonze, and G.-M. Rignanese, Comput. Phys. Commun. **226**, 39 (2018).

[57] J. P. Perdew and Y. Wang, Phys. Rev. B **33**, 8800 (1986).

[58] J. P. Perdew, K. Burke, and M. Ernzerhof, Phys. Rev. Lett. **77**, 3865 (1996).

[59] X. Gonze, Phys. Rev. A **52**, 1096 (1995).

[60] X. Gonze and C. Lee, Phys. Rev. B **55**, 10355 (1997).

[61] X. Gonze, Phys. Rev. B **55**, 10337 (1997).

[62] S. Baroni, S. D. Gironcoli, A. D. Corso, and P. Giannozzi, Rev. Mod. Phys. **73**, 515 (2001).

[63] A. Belsky, M. Hellenbrandt, V. L. Karen, and P. Luksch, Acta Crystallogr. Sect. B: Struct. Sci. **58**, 364 (2002).

[64] S. Gražulis, D. Chateigner, R. T. Downs, A. F. Yokochi, M. Quirós, L. Lutterotti, E. Manakova, J. Butkus, P. Moeck, and A. Le Bail, J. Appl. Crystallogr. **42**, 726 (2009).

[65] E. Blokhin and P. Villars, The pauling file project and materials platform for data science: From big data toward materials genome, in *Handbook of Materials Modeling: Methods: Theory and Modeling* (Springer, Cham, Switzerland, 2020), pp. 1837–1861.

[66] J. E. Saal, S. Kirklin, M. Aykol, B. Meredig, and C. Wolverton, JOM **65**, 1501 (2013).

[67] P. Giannozzi, S. Baroni, N. Bonini, M. Calandra, R. Car, C. Cavazzoni, D. Ceresoli, G. L. Chiarotti, M. Cococcioni, I. Dabo *et al.*, J. Phys.: Condens. Matter **21**, 395502 (2009).

[68] G. Graziano, J. Klimes, F. Fernandez-Alonso, and A. Michaelides, J. Phys.: Condens. Matter **24**, 424216 (2012).

[69] G. Prandini, A. Marrazzo, I. E. Castelli, N. Mounet, and N. Marzari, npj Comput. Mater. **4**, 72 (2018).

[70] J. J. Mortensen, A. H. Larsen, M. Kuisma, A. V. Ivanov, A. Taghizadeh, A. Peterson, A. Haldar, A. O. Dohn, C. Schäfer, E. Ö. Jónsson *et al.*, J. Chem. Phys. **160**, 092503 (2024).

[71] E. Kucukbenli, M. Monni, B. I. Adetunji, X. Ge, G. A. Adebayo, N. Marzari, S. de Gironcoli, and A. Dal Corso, arXiv:1404.3015.

[72] A. Jain, S. P. Ong, G. Hautier, W. Chen, W. D. Richards, S. Dacek, S. Cholia, D. Gunter, D. Skinner, G. Ceder, and K. A. Persson, APL Mater. **1**, 011002 (2013).

[73] See Supplemental Material at http://link.aps.org/supplemental/10.1103/dj5c-d24m for the data used to produce the Figs. 1, 3–6 and Table II.

[74] The eggbox effect in a planewave basis set is solely due to the computation of the exchange-correlation energy (and potential) on a discrete grid. It is quite small, usually less than 1 mHa per atom. See Appendix C.1 of the Ph.D. thesis of ph. Ghosez, http://www.phythema.ulg.ac.be/webroot/misc/books/PhD-Ph.Ghosez.pdf. When also the kinetic energy is computed on a discrete grid, like in Ref. [75] online, the eggbox effect is larger.

[75] D. Roller, A. M. Rappe, L. Kronik, and O. Hellman, J. Chem. Theory Comput. **19**, 3889 (2023).

[76] H. Jónsson, G. Mills, and K. W. Jacobsen, Nudged elastic band method for finding minimum energy paths of transitions, in *Classical and Quantum Dynamics in Condensed Phase Simulations* (World Scientific, 1998), pp. 385–404.

[77] G. Henkelman and H. Jónsson, J. Chem. Phys. **113**, 9978 (2000).

[78] G. Henkelman, B. P. Uberuaga, and H. Jónsson, J. Chem. Phys. **113**, 9901 (2000).

[79] V. Ásgeirsson, B. O. Birgisson, R. Bjornsson, U. Becker, F. Neese, C. Riplinger, and H. Jónsson, J. Chem. Theory Comput. **17**, 4929 (2021).

[80] S. Amisi, E. Bousquet, K. Katcho, and P. Ghosez, Phys. Rev. B **85**, 064112 (2012).

[81] H. Djani, E. Bousquet, A. Kellou, and P. Ghosez, Phys. Rev. B **86**, 054107 (2012).

[82] M. Veithen and P. Ghosez, Phys. Rev. B **65**, 214302 (2002).

[83] P. Ghosez, X. Gonze, and J.-P. Michenaud, Ferroelectrics **206**, 205 (1998).